C. R. Physique 15 (2014) 190–199

Contents lists available at ScienceDirect

Comptes Rendus Physique

www.sciencedirect.com

Electron microscopy / Microscopie électronique

# Shaping electron beams for the generation of innovative measurements in the (S)TEM

## *Réaliser des mesures originales et innovantes en adaptant le faisceau d'électrons d'un (S)TEM*

Jo Verbeeck [a,*], Giulio Guzzinati [a], Laura Clark [a], Roeland Juchtmans [a], Ruben Van Boxem [a], He Tian [a], Armand Béché [a], Axel Lubk [a,b], Gustaaf Van Tendeloo [a]

[a] *EMAT, University of Antwerp, Groenenborgerlaan 171, 2020 Antwerp, Belgium*
[b] *Triebenberglabor, University of Dresden, Zum Triebenberg 1, 01062 Dresden, Germany*

ARTICLE INFO

*Article history:*
Available online 31 January 2014

*Keywords:*
Vortex beam
Transmission Electron Microscopy
Angular momentum
Topological Charge
Nanomanipulation
Magnetic properties

*Mots-clés :*
Vortex
Microscopie électronique en transmission
Moment angulaire
Charge topologique
Nanomanipulation
Propriétés magnétiques

ABSTRACT

In TEM, a typical goal consists of making a small electron probe in the sample plane in order to obtain high spatial resolution in scanning transmission electron microscopy. In order to do so, the phase of the electron wave is corrected to resemble a spherical wave compensating for aberrations in the magnetic lenses. In this contribution, we discuss the advantage of changing the phase of an electron wave in a specific way in order to obtain fundamentally different electron probes opening up new applications in the (S)TEM. We focus on electron vortex states as a specific family of waves with an azimuthal phase signature and discuss their properties, production and applications. The concepts presented here are rather general and also different classes of probes can be obtained in a similar fashion, showing that electron probes can be tuned to optimize a specific measurement or interaction.



RÉSUMÉ

Dans un microscope électronique à transmission, l'objectif le plus courant est de focaliser le plus finement possible la sonde d'électrons primaires dans le plan de l'échantillon, afin d'obtenir la meilleure résolution spatiale en STEM (*Scanning Transmission Electron Microscopy*). Dans ce but, l'utilisation d'un correcteur de Cs sonde est particulièrement importante pour s'approcher d'une onde sphérique idéale. Dans cet article, nous discuterons des avantages que peuvent présenter les modifications spécifiques de cette phase pour créer des sondes d'électrons totalement différentes, ouvrant le champ à des applications originales en STEM. Nous insisterons, en particulier, sur les sondes d'électrons de type « vortex », une famille d'ondes possédant une signature azimutale de phase, dont nous décrirons l'obtention, les propriétés et différentes utilisations. Ces concepts très généraux peuvent être étendus à différents types de sondes, alors optimisées pour une mesure ou une intéraction particulière.



* Corresponding author.

1631-0705/$ – see front matter 
http://dx.doi.org/10.1016/j.crhy.2013.09.014

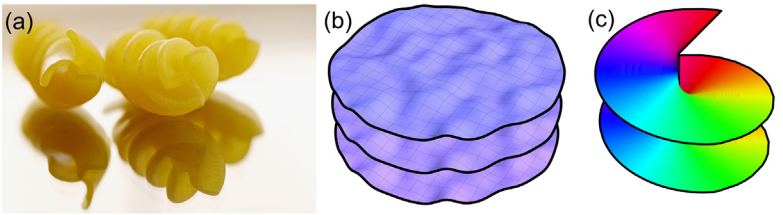


**Fig. 1.** (Colour online.) (a) A common example of the $\ell = 3$ wavefront structure, demonstrated in fusilli pasta [17]. (b) Equiphase surfaces of a plane wave with random smooth distortions. (c) Equiphase surface of an $\ell = 1$ vortex beam.

## 1. Introduction

It was recently predicted, and experimentally demonstrated, that changing the fundamental structure of electron wavefronts can imbue them with a number of particular properties, enabling new functionality within a conventional transmission electron microscope (TEM) [1–3]. These restructured electron beams have continuous helical wavefronts, and are thus referred to as electron vortex beams [2,3]. Accordingly, the electron probability current follows a spiralling path, propagating along the optical axis, with an azimuthal momentum component [4].

Vortices occur across a broad variety of physics subfields—in classical fluid mechanics, superconductors, ocean tides and collective human behavior [5–9]. Screw-type phase singularities were first discussed as a ubiquitous feature of wave physics in 1974 [10], followed by studies progressing into the deliberate production of optical beams with the azimuthal phase dependence, in the work of Vaughan and Willetts [11] and Bazhenov et al. [12].

A simple vortex beam can be described by $\Psi \propto f(r)\exp(\mathrm{i}\ell\varphi)\exp(\mathrm{i}k_z z)$, where $(r, \varphi, z)$ are the cylindrical coordinates, and $k_z$ is the forward momentum of the beam. The order of the vortex is $\ell$, wherein the phase changes by $2\pi\ell$ in a circuit around the vortex core. In this single vortex case, $\ell$ is equal to the winding number [13], a key parameter describing the field vorticity. The vortex order is also related to the orbital angular momentum (OAM) of the beam, a property that has been of much interest in the field of singular optics [14–16].

To visualize such beams easily, the wavefronts of an $\ell = \pm 3$ vortex beam are of the same structure as a piece of fusilli pasta, as illustrated in Fig. 1a.

Along the axis of a vortex beam, all phases meet, and as such there is an indeterminacy in the phase along the axis, called a phase singularity, or in 3D, a vortex line [18,19]. The screw-structured phase singularity was first discussed by Nye and Berry in 1974 [10]. As a consequence of the meeting of phases, the intensity on the axis is forced to zero by destructive interference. Indeed, this is a key indicator of a vortex beam, accessible without phase measurement techniques; the central zero-intensity of a vortex beam remains present throughout propagation, while in a non-vortex, hollow beam, the central minimum will disappear over propagation due to diffractive spreading. A further result of the phase singularity is that a vortex beam is topologically distinct from a planar or spherical wavefront—no continuous stretching or warping can cause the creation of a vortex wavefront from planar or spherical surfaces, as illustrated in Fig. 1 [13].

Following the development of vortex beam theory throughout the later part of the 20th century, vortex beams of photons, electrons, and acoustic waves have now found practical applications in a broad range of fields. They have significant applications in atomic and molecular manipulation, trapping and rotation, including work with Bose–Einstein condensates [20,21]. They have been demonstrated across a broad range of the electromagnetic spectrum [22–25]. Acoustic vortex beams have been studied by a number of groups [26,27], while optical vortex beams are finding further application beyond typical optics studies in astrophysics [28], and in telecommunications [29,30,20].

## 2. Vortex beam properties

The simplest scalar wave function solution describing particles with orbital angular momentum (OAM) is the *Bessel beam* [31],

$$\Psi_\ell(r, \varphi, z) = \mathrm{e}^{\mathrm{i}k_z z}\mathrm{e}^{\mathrm{i}\ell\varphi}\mathrm{J}_\ell(k_\perp r) \tag{1}$$

which is an exact solution of the time-independent Schrödinger equation and an eigenvector of the cylindrical free space Hamiltonian, the longitudinal momentum $p_z$, the transverse momentum $p_\perp = \mathrm{i}\hbar\sqrt{\partial_x^2 + \partial_y^2}$, and the OAM $L_z = -\mathrm{i}\hbar\partial_\varphi$. Here, $\hbar\ell$ is the OAM eigenvalue, $\mathrm{J}_\ell$ is the $\ell$-th cylindrical Bessel function of the first kind, and $k_\perp$ is the transverse momentum of the vortex state. The transverse momentum $k_\perp$ is the eigenvalue of the operator $p_\perp$. Fig. 2a shows the Fourier transform of a Bessel beam, which is, up to normalization, a Dirac delta ring multiplied by a phase factor. Bessel beams are the formal basis functions of the cylindrical Schrödinger equation, and a single state as in Eq. (1) cannot be realized in experiments much the same as a true plane wave cannot exist in experiments. The Bessel beam intensity profiles (modulus squared of the wave function in Eq. (1)) for several $\ell$ are shown in Fig. 2b. A circular aperture with a spiral phase structure contains a single $\ell$ mode Bessel beam superposition of the following form:

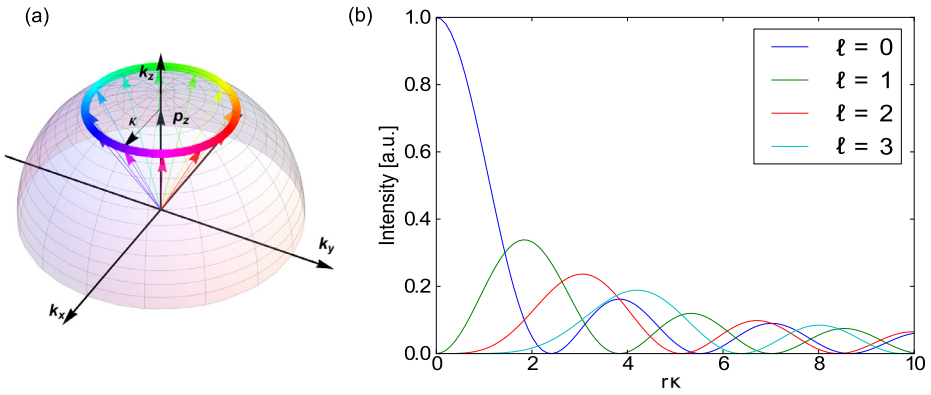


**Fig. 2.** (Colour online.) (a) Fourier space representation of a Bessel beam $\Psi_1$ (see Eq. (1)). The radius of the ring is equal to the transverse momentum $\kappa$. (b) Radial intensity for different topological charges. For $l = 0$, we obtain the well-known Airy disc; for $l \neq 0$, doughnut-like intensity distributions are obtained.

$$\Psi \propto \mathrm{e}^{\mathrm{i}\ell\varphi} \int_0^{k_\perp^{\max}} \mathrm{d}k_\perp k_\perp \mathrm{J}_\ell(k_\perp r) \tag{2}$$

containing a sum of $k_\perp$ eigenstates up to a maximum $k_\perp^{\max}$ proportional to the radius of the aperture. For $\ell = 0$, we recover the typical Airy disc while for other values of $\ell$ a slightly broader vortex beam is obtained for the same $k_\perp^{\max}$. The smallest electron vortex beam diameter obtained thus far had a diameter of 1.2 Å [32].

The above solutions of the Schrödinger equation will change significantly in a magnetic field, and depending on the exact form of the external field, propagation dynamics and angular momentum will change [33]. Fully relativistic solutions have been investigated as well by several authors, but the free-space relativistic effects have been found to be negligible [34,35].

A scalar electron vortex possesses a topological charge defined by its winding number:

$$\ell = \frac{1}{2\pi} \oint \mathrm{d}\phi = \frac{1}{2\pi} \oint \frac{\nabla\Psi}{\Psi} \cdot \mathrm{d}\boldsymbol{s} \tag{3}$$

This distinguishes a vortex wave from a plane wave. Lubk et al. showed that the propagation of an electron vortex is *topologically protected*, *i.e.* a vortex probe will not delocalize as rapidly as a conventional $\ell = 0$ probe [13,36]. One must be careful relating the winding number in Eq. (3) directly to the OAM as they are only equal in the case of an OAM eigenstate, which means the electron density is radially symmetric around the phase dislocation. For better clarity, we will suppose in the following that this condition is always fulfilled.

Vortex beam states as discussed in Eq. (1) are eigenvectors of the OAM operator for which:

$$\langle L_z \rangle = \hbar\ell \tag{4}$$

The current experimental record for electron vortices' OAM is $\ell = 100$, although this was in the weak higher diffraction orders of a holographic fork aperture [37]. Translating and tilting the OAM axis with respect to the symmetry axis results in a change in the expectation value of $L_z$ and the decomposition in its components [38–40]. In scattering experiments, this is an important detail to take into account [41,13,32]. Additionally, a scattered electron wave may have its principal OAM axis rotated by the scattering event, in which case further care needs to be taken to calculate and measure the outgoing electron wave [42].

Bessel beams as in Eq. (1) show a spiralling current approximately equal to [1]:

$$\boldsymbol{j}(r) \approx \rho(r)\left(k_z \boldsymbol{e}_z + \frac{\hbar\ell}{r}\boldsymbol{e}_\varphi\right) \tag{5}$$

This current lies perpendicular to the (spiralling) wave front's equiphase surface. Figs. 1b–c compare a continuously distorted wavefront's equiphase surface to that of a vortex beam. It is immediately evident that one cannot be simply transformed into the other without introducing a discontinuity in both the current and the phase surface.

The electromagnetic fields of a Bessel beam are given by [43]:

$$\boldsymbol{E}(r) \propto -r\left[\mathrm{J}_\ell^2(k_\perp r) - \mathrm{J}_{\ell-1}(k_\perp r)\mathrm{J}_{\ell+1}(k_\perp r)\right]\boldsymbol{e}_r \tag{6a}$$

$$\boldsymbol{B} = B_\varphi \boldsymbol{e}_\varphi + B_z \boldsymbol{e}_z \tag{6b}$$

$$B_\varphi \propto r\left[\mathrm{J}_\ell^2(k_\perp r) - \mathrm{J}_{\ell-1}(k_\perp r)\mathrm{J}_{\ell+1}(k_\perp r)\right] \tag{6c}$$

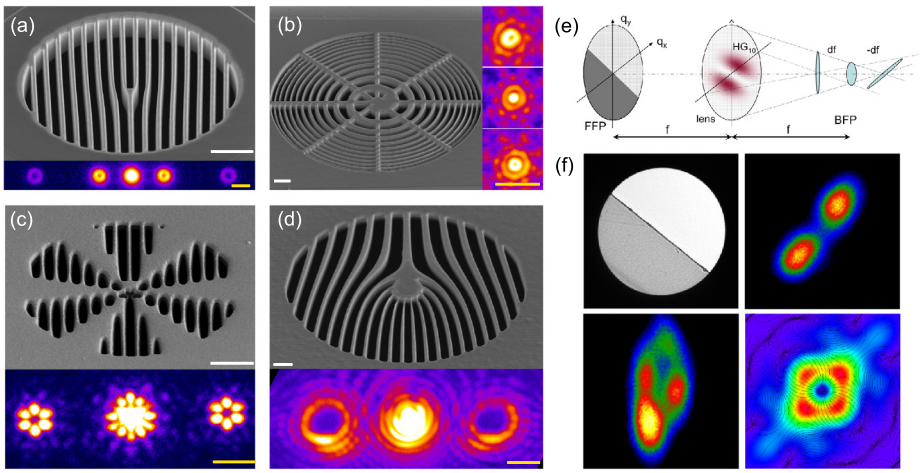


**Fig. 3.** (Colour online.) Examples of holographic reconstruction: SEM micrographs of the holograms are shown alongside the beams they produce when used in a TEM. The hologram images have a 2-μm white scalebar, the beam intensities have a 20-nm yellow scalebar. (a) Example of $\ell = 1$ fork hologram. The $\ell = 0$ beam is visible in the center, with the first sidebands of $\ell = \pm 1$ and the higher order with $\ell = \pm 3$ at the border of the image. (b) Spiral hologram generated by the interference of an $\ell = 1$ vortex beam with a spherical wave. The probes shown on the side are separated along the beam axis. (c) The target wave used was the flower-shaped superposition of $\ell = 3$ and $\ell = -3$ vortex modes. (d) Higher-order $\ell = \pm 9$ vortex modes. (e) Diagram of the vortex generation through mode conversion. The Hilbert phase plate in the front focal plane of a lens introduces a phase shift of $\pi$ in the incident plane wave, generating a beam with two lobes, which is then converted into a vortex beam by introducing astigmatism. (f) Top: Shadow image of the phase plate and resulting beam produced by the phase shift. Bottom: Experimentally generated vortex beam and simulation of the ideal result. Despite the distortions, attributed to the partial absorption by the phase plate, the central phase singularity is clearly visible. (e) and (f) from Schattschneider et al., 2012 [45].

$$B_z \propto \frac{\ell}{r} \int_r^\infty \mathrm{J}_\ell^2(k_\perp r')\,\mathrm{d}r' \tag{6d}$$

The magnetic field in the $z$ direction, $B_z$, peaks at the center of the vortex. Note that considering a more realistic wave packet will add fringe fields which do not appear in the unlocalized and unnormalized Bessel beam case. It will also remedy the fact that in the above expression, $B_z$ is always positive and there are no returning field lines.

Another interesting feature of electron vortex states (as in Eq. (1)) is their magnetic moment, $\boldsymbol{\mu}$, which is proportional to the OAM [33]:

$$\boldsymbol{\mu} = \frac{e\hbar}{2} \frac{\int \boldsymbol{r} \times \boldsymbol{j}\,\mathrm{d}V}{\int \rho\,\mathrm{d}V} = \ell \mu_B \boldsymbol{e}_z \tag{7}$$

This can be arbitrarily tuned by changing the OAM of the beam.

## 3. Vortex creation

A variety of methods, many derived from optics, have been used to create electron vortex beams. The purpose of these techniques is the controlled manipulation of the phase of the electron wave in order to generate the characteristic singularity. It should be noted that these methods are often entirely general, and can be used to obtain many other types of waves, such as electron Airy beams that have recently gained interest [44].

Holographic reconstruction has so far been the most common method for the production of electron vortex beams. In conventional electron holography, one interferes the wave transmitted through a sample with a reference wave, creating a hologram that encodes the phase and amplitude in the interference pattern. In holographic reconstruction one makes use of a computer generated hologram in order to reproduce a target wave with a desired amplitude and phase profile. The hologram is calculated by superimposing the target function ($\Psi \propto \exp(\mathrm{i}\ell\varphi)$ for a vortex beam) with a reference wave such as a tilted plane wave of the form $\exp(\mathrm{i}k_x x)$. The hologram is binarized by using a threshold which is needed as a true amplitude modulation in TEM is very difficult to realise. The binary hologram can then be manufactured through standard nanofabrication techniques such as electron beam lithography (EBL), electron beam-induced deposition (EBID) or most commonly milled with a focused ion beam (FIB) instrument on a metallic thin film of heavy, strongly scattering metals such as platinum or gold [3,37].

When such a hologram is inserted in the TEM and illuminated with a sufficiently coherent electron beam, the desired vortex beam can be observed in the far field of the mask hologram. The diffraction pattern contains a central spot from the reference wave and two sidebands with one having the desired waveform and the other being its complex conjugate (see Fig. 3). The binarization of the mask introduces higher diffraction orders with higher OAM that can be seen at higher distance from the center of the pattern. The ensemble of these diffracted beams forms a one-dimensional vortex lattice

(see Fig. 3a). This method allows for several variations by changing either the reference, or the target wave. If a spherical reference wave is used instead of a plane wave, the generated hologram assumes a spiral shape and the various vortex orders are separated longitudinally along the beam axis as in Fig. 3b. This approach is especially suited for scanning transmission electron microscopy (STEM) since one vortex order can be focused on the sample at a given time and therefore give spatial information, while the other vortex probes are out of focus and provide only a background signal [46]. Atomically resolved STEM images with vortex probes were obtained this way [46]. If the target wave is changed, the holographic method allows the generation of superpositions of vortex beams [47,48] (Fig. 3c), beams with higher-order topological charge [37,49] (Fig. 3d) and electron Airy beams [44]. This last type of beam is of note, as the target phase is completely different from that of a vortex and its feasibility demonstrates the flexibility of holographic reconstruction.

The phase of an electron beam is also influenced by electric and magnetic fields, such as the mean inner potential of a thin sample which induces a phase shift in an electron wave traveling through it. A weak potential $V_0$ will induce a phase shift on the electron beam of $\Delta\phi = \frac{\pi}{2\lambda E}\int V_0(\vec{r})\,\mathrm{d}z$ where $\lambda$ is the electron wavelength and $E$ is its energy. This has been exploited in the fabrication of phase plates for electron microscopy with the purpose of enhancing the contrast in weakly scattering samples [50,51]. Examples of such phase plates are Zernike phase plates [52,53], which induce a phase shift of $\pi/2$ in scattered waves for better phase contrast and are realized by a thin carbon film with a hole drilled in the centre [50], or Hilbert phase plates, which produce a topological contrast by inducing a phase shift of $\pi$ between the lobes of a beam and are made of a semicircular thin film [51]. Electrostatic Boersch phase plates exist as well, creating a phase shift with a microfabricated electrostatic lens [54].

In order to produce a vortex wave, a spiral phase plate is needed and can in principle be produced using the same principles as the simpler phase plates discussed above. An approximate spiral phase plate, given by a spontaneous staircase arrangement of graphite thin films in a sample, was indeed used in the first demonstration that electron vortex beams do occur in a TEM [2].

However, such a phase plate is extremely challenging to produce. If made out of carbon and designed for an electron beam with a kinetic energy of 300 keV, the required thickness would be about 80 nm at the thickest point and should then be stepped gradually down to 0 nm. This degree of thickness control is extremely hard to reach with current technology, and the resulting object would suffer from a higher degree of contamination and radiation damage as compared to the binary holograms [50]. Using heavier elements would require an even lower thickness and scattering would further complicate the electron interaction. It is worth noting that these phase plates have to be designed for a specific acceleration voltage of the TEM, as the acquired phase shift depends strongly on it.

Hilbert phase plates have also been used in combination with a controlled level of astigmatism to produce electron vortices [45], through the so-called *mode-conversion* process [14,55] (Fig. 3e, f).

Despite the challenges presented in producing an electron phase plate, direct manipulation of the phase is performed when correcting the aberration of electron lenses. In fact, aberration correctors are designed to generate a phase plate to compensate for the aberration phase shifts of a lens system, but also allow the free tuning of the individual aberrations to obtain a desired phase plate. Indeed, while a high degree of aberration has been shown to induce a diffraction catastrophe that generates a vortex lattice [56], it has been shown that a careful tuning of different orders of astigmatism, together with an angle-limiting annular aperture, can be used to produce a single high-intensity vortex beam [57].

Magnetic fields also induce a phase shift in an electron wave through the Aharonov–Bohm effect. Indeed two different electron paths are phase shifted with respect to each other by $\Delta\phi = \oint \boldsymbol{A}\cdot\mathrm{d}\boldsymbol{s} = \int_{\Sigma}\boldsymbol{B}\cdot\mathrm{d}\boldsymbol{S}$. The Aharonov–Bohm phase shift is commonly exploited through electron holography to measure the in-plane component of the magnetization [58]. The fabrication of magnetic phase plates for contrast enhancement through the Aharonov–Bohm phase is also currently under study [59]. It has been shown that there is an intimate link between the Aharonov–Bohm effect and electron vortex beams [33] and that the characteristic field of a magnetic monopole would introduce an azimuthal phase shift that would turn a plane wave into a vortex with an OAM eigenvalue equal to the monopole's magnetic charge [60,1]. Recently, it has been shown how a magnetic monopole field can be approximated by the end of a thin magnetic needle, providing a vortex beam generation mechanism that works independently of the electron kinetic energy. This method can produce electron vortex beams with high current and potentially very high OAM [61,62].

After this discussion of the techniques devised for the production of vortex beams, it is worth noting that electron vortices are also created in the inelastic collisions between the incident electrons and the atoms of a sample. The exchange of angular momentum in the interaction puts the inelastically scattered electron in a mixed state that naturally contains vortices [63]. In that sense, electron vortices have always existed and are nearly impossible to avoid.

## 4. Applications

Electron vortex beams have great potential in a number of applications, some of which have been demonstrated experimentally and others which thus far remain theoretical concepts.

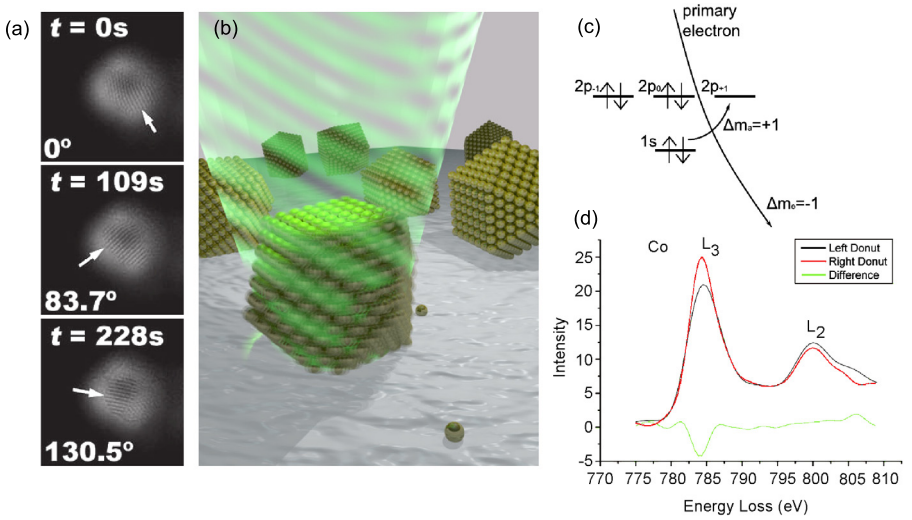


**Fig. 4.** (Colour online.) (a) Time series of atomic resolution images of a 3-nm gold particle illuminated by an $\ell = 1$ vortex beam. The arrow denotes the direction of the (111) planes. From Verbeeck et al., 2013. (b) Artistic representation of a gold nanoparticle illuminated by a vortex beam. (c) Scheme of the electronic transition under consideration, $1s \rightarrow 2p_{+1}$ showing a different cross section for the $\Delta m_1$ transition when illuminated with a $\ell = +1$ or a $\ell = -1$ beam. (d) Measured EELS signal from left and the right sideband showing a clear difference on the $L_{2,3}$ edges. From Verbeeck et al., 2013.

### *4.1. Nanomanipulation*

As stated above, electron vortex beams carry a well-defined orbital angular momentum of $\ell\hbar$ per electron. When scattered at a particle though, radial symmetry is broken and OAM is no longer a good quantum number [41]. Consequently, transfer of OAM between the vortex and the particle is possible [21].

This effect is demonstrated by Verbeeck et al. in Ref. [21], where a gold nanoparticle with a diameter of 3 nm is illuminated by an $\ell = \pm 1$ vortex of comparable size. By looking at the (111) planes of the gold particle in time, a rotation of 0.01 rad/s is measured, as visible in Fig. 4a. The sense of this rotation is determined by the sign of $\ell$, demonstrating that the rotation of the gold particle is a consequence of the vortex character of the electrons. It was calculated numerically, that an OAM of about $0.1\hbar$ per electron is transferred to the crystal. The size of this transfer depends crucially on the orientation of the particle with respect to the beam. Neglecting friction, this would result in a linearly increasing rotational velocity of approximately $10^{14}$ rad/s$^2$ for a typical beam current of 50 pA, which would cause the particle to disintegrate very rapidly. Incorporating friction however, a stationary rotation velocity of 0.037 rad/s is calculated, much closer to the observed value.

This experiment clearly shows that electrons carrying OAM can be used to rotate nanoparticles and could be a useful complement to atomic force microscopy techniques for manipulating nanoparticles. In addition, electron vortex beams offer a new tool for studying rotational friction of nanoparticles [21].

### *4.2. Energy-loss magnetic circular dichroism (EMCD)*

Dichroism describes the variable absorption cross-section of a material, dependent on the polarisation of the incoming photon. In X-ray magnetic circular dichroism (XMCD), first observed on the K-edge signal of iron [64], the absorption cross-section depends on the angle between the helicity of a circularly polarized photon and the magnetization of a ferromagnetic or paramagnetic material. By looking at the energy-loss spectrum of the photons, information about the magnetic ordering of the material can be obtained. Recently Schattschneider et al. demonstrated that the same can be done using electrons (EMCD) by exploiting the equivalence between the polarization vector $\boldsymbol{\epsilon}$ in X-ray absorption and the momentum transfer $\hbar\boldsymbol{q}$ in electron scattering [65].

Verbeeck et al. suggested another EMCD setup for mapping the spin-polarized $2p \rightarrow 3d$ electronic transitions from a thin homogeneously magnetized ferromagnetic iron sample [3]. These transitions can transfer OAM to an inelastically scattered electron if an asymmetry between the inelastic transition of $\Delta\ell = 1$ and $\Delta\ell = -1$ exists. This asymmetry is always present in atoms carrying a magnetic moment mediated by a complex spin–orbit coupling of the atomic states [66]. As a consequence, the inelastic electrons carry a net excess of OAM with a different sign for the $L_2$ and $L_3$ excitations in electron energy-loss spectroscopy. This imbalance in OAM versus energy loss is measured by placing an $\ell = 1$ fork hologram in the selected area plane and then placing the spectrometer entrance aperture in the center of the sidebands. The difference in the spectra obtained in the two sidebands is then due only to the magnetic transitions, as shown in Fig. 4d, much in the same way as in XMCD. The advantage of this method over XMCD however, is that atomic resolution is feasible with electron vortices. Preliminary related experiments indicate that this indeed seems possible [67] although a sub-optimal signal to noise ratio makes the interpretation difficult.

### 4.3. Vortex electron energy-loss spectroscopy for near-field mapping of magnetic plasmons

When passing through or moving in the vicinity of a material, an electron can excite plasmons in a material. Recording the energy lost in this process by means of electron energy-loss spectroscopy (EELS), a map of the electrical part of the local plasmonic response of nanomaterials can be reconstructed [68,69]. One could expect that a vortex electron, carrying a magnetic moment of $\ell\mu_B$, could be used to probe the magnetic part of the local plasmonic response of a particle down to the nanometer scale.

The magnetic response of a split-ring resonator (SRR) is calculated using a semi-classical approach by Mohammadi et al. [70]. Conventional finite-difference time domain (FDTD) calculations were performed for calculating normal EELS scattering probabilities in which the electric charge is replaced by an effective magnetic charge. It was shown that the magnetic component of the EELS signal is of the same order as the conventional EELS signal. This opens up the route for using vortex beams as a tool for mapping the magnetic response of nano-particles and could be of great importance in the search for artificial metal nanostructures with a large magnetic response in the visible-light spectrum. Such nanostructures could be applicable to, for example, perfect lenses and optical cloaking [71,72].

### 4.4. Spin–orbit conversion

In the following a short outline is given of how a space-variant Wien filter can be used as a spin-polarizer when using electron vortices following Karimi et al. [73]. Considering a spin-unpolarized vortex beam moving along the $z$-axis with topological charge $\ell$, $\Psi = \frac{1}{\sqrt{2}}(|\uparrow, \ell\rangle + |\downarrow, \ell\rangle)$, where the spin is taken along the propagation axis. When moving through a magnetic field of the form $\boldsymbol{B}(r, \phi, z) = B_0(r)(\cos(\alpha(\phi)), \sin(\alpha(\phi)), 0)$, with $\alpha(\phi) = m\phi + \beta$ and $\phi$, being the azimuthal coordinate, part of the spin-up component will flip to a spin-down state and vice versa. Depending on the initial spin-state, the spin-flipped part of the wave function will gain or lose an amount of OAM equal to $m\hbar$, that is [73]:

$$\begin{aligned} |\uparrow, \ell\rangle &\rightarrow \cos(\delta/2)|\uparrow, \ell\rangle + \mathrm{i}\,\mathrm{e}^{\mathrm{i}\beta}\sin(\delta/2)|\downarrow, \ell + m\rangle \\ |\downarrow, \ell\rangle &\rightarrow \cos(\delta/2)|\downarrow, \ell\rangle + \mathrm{i}\,\mathrm{e}^{-\mathrm{i}\beta}\sin(\delta/2)|\uparrow, \ell - m\rangle \end{aligned} \tag{8}$$

where $\delta = gL/R_c$ and $R_c$ is the cyclotron radius. It can be seen from Eq. (8) that when $\ell = \pm m$, part of the vortex beam will lose all of its OAM and that this part will be spin-polarized. When propagating to the far-field, the $\ell = 0$ component of the electron wave will cause a finite amount of intensity to be present in the centre of the beam, while the OAM-containing components will not. By placing a small aperture in this plane, the $\ell = 0$ part of the beam can be selected, resulting in a spin-polarized beam.

According to Karimi et al., the beam can have a degree of polarization up to 97.5%, while maintaining an intensity of two orders of magnitude greater than conventional spin-polarized electron sources [73]. Although exchange effects are seen to be negligible in current TEM experiments, a high-intensity polarized electron source would be a breakthrough [13].

## 5. Outlook and conclusion

Electron waves provide more flexibility in amplitude and phase than the small subset of plane wave and spherical wave which are commonly used in a TEM. In this review, we have shown how the new class of vortex waves with an azimuthal phase signature can expand the possibilities in TEM beyond the current state of the art. We have shown the peculiar and specific properties of these vortex beams as well as a wide range of methods by which they can be produced. As the creation of these waves is relatively new, their applications are just starting to emerge. The most promising application is undoubtedly the appearance of magnetic information in EELS, which offers the potential of probing magnetic moments at the atomic scale. Compared to optical vortices which came around in the 90s with many applications maturing only now, electron vortices are new and the field is still rapidly expanding. As with all technique developments in TEM, the field will only flourish when it provides unique and valuable information in a user friendly way. Perhaps more important than electron vortices is the paradigm shift from making small electron probes towards optimizing the wave function in order to obtain maximum selectivity on a given property of the sample. In other words: what wave function will lead to the best answer to a specific materials science question? In this respect, we profit from the increased flexibility that e.g. an aberration corrector offers, but compared to the programmable phase plates that are common in light optics, there is still ample room for improving this flexibility in the future.

## References

[1] Konstantin Yu. Bliokh, Yury P. Bliokh, Sergey Savel'ev, Franco Nori, Semiclassical dynamics of electron wave packet states with phase vortices, Phys. Rev. Lett. 99 (Nov 2007) 190404, http://dx.doi.org/10.1103/PhysRevLett.99.190404, URL http://link.aps.org/doi/10.1103/PhysRevLett.99.190404.

[2] Masaya Uchida, Akira Tonomura, Generation of electron beams carrying orbital angular momentum, Nature (ISSN 0028-0836) 464 (7289) (April 2010) 737–739, http://dx.doi.org/10.1038/nature08904, URL http://www.nature.com/nature/journal/v464/n7289/abs/nature08904.html.

[3] J. Verbeeck, H. Tian, P. Schattschneider, Production and application of electron vortex beams, Nature (ISSN 1476-4687) 467 (7313) (September 2010) 301–304, http://dx.doi.org/10.1038/nature09366, URL http://www.ncbi.nlm.nih.gov/pubmed/20844532.

[4] P. Schattschneider, J. Verbeeck, Theory of free electron vortices, Ultramicroscopy (ISSN 0304-3991) 111 (9–10) (2011) 1461–1468, http://dx.doi.org/10.1016/j.ultramic.2011.07.004, URL http://www.sciencedirect.com/science/article/pii/S0304399111001811.

[5] P.G. Saffman, Vortex Dynamics, Cambridge Monographs on Mechanics and Applied Mathematics, Cambridge University Press, ISBN 9780521420587, 1992, URL http://books.google.be/books?id=ksktDE0yVzcC.

[6] Ernst Helmut Brandt, Vortices in superconductors, Physica C, Supercond. (ISSN 0921-4534) 369 (1–4) (2002) 10–20, http://dx.doi.org/10.1016/S0921-4534(01)01215-1, URL http://www.sciencedirect.com/science/article/pii/S0921453401012151.

[7] William Whewell, Essay towards a first approximation to a map of cotidal lines, Philos. Trans. R. Soc. Lond. 123 (1833) 147–236, URL http://rstl.royalsocietypublishing.org/content/123/147.full.pdf+html.

[8] J.F. Nye, J.V. Hajnal, J.H. Hannay, Phase saddles and dislocations in two-dimensional waves such as the tides, Proc. R. Soc. Lond. Ser. A, Math. Phys. Sci. 417 (1852) (1988) 7–20, http://dx.doi.org/10.1098/rspa.1988.0047, URL http://rspa.royalsocietypublishing.org/content/417/1852/7.abstract.

[9] Jesse L. Silverberg, Matthew Bierbaum, James P. Sethna, Itai Cohen, Collective motion of humans in mosh and circle pits at heavy metal concerts, Phys. Rev. Lett. 110 (May 2013) 228701, http://dx.doi.org/10.1103/PhysRevLett.110.228701, URL http://link.aps.org/doi/10.1103/PhysRevLett.110.228701.

[10] J.F. Nye, M.V. Berry, Dislocations in wave trains, Proc. R. Soc. Lond. Ser. A, Math. Phys. Sci. 336 (1605) (1974) 165–190, http://dx.doi.org/10.1098/rspa.1974.0012, URL http://rspa.royalsocietypublishing.org/content/336/1605/165.abstract.

[11] J.M. Vaughan, D.V. Willetts, Temporal and interference fringe analysis of $TEM_{01}^{*}$ laser modes, J. Opt. Soc. Am. 73 (8) (Aug 1983) 1018–1021, http://dx.doi.org/10.1364/JOSA.73.001018, URL http://www.opticsinfobase.org/abstract.cfm?URI=josa-73-8-1018.

[12] V.Yu. Bazhenov, M.S. Soskin, M.V. Vasnetsov, Screw dislocations in light wavefronts, J. Mod. Opt. 39 (5) (1992) 985–990, http://dx.doi.org/10.1080/09500349214551011, URL http://www.tandfonline.com/doi/abs/10.1080/09500349214551011.

[13] Axel Lubk, Laura Clark, Giulio Guzzinati, Jo Verbeeck, Topological analysis of paraxially scattered electron vortex beams, Phys. Rev. A 87 (Mar 2013) 033834, http://dx.doi.org/10.1103/PhysRevA.87.033834, URL http://link.aps.org/doi/10.1103/PhysRevA.87.033834.

[14] L. Allen, M.W. Beijersbergen, R.J.C. Spreeuw, J.P. Woerdman, Orbital angular momentum of light and the transformation of Laguerre–Gaussian laser modes, Phys. Rev. A 45 (Jun 1992) 8185–8189, http://dx.doi.org/10.1103/PhysRevA.45.8185, URL http://link.aps.org/doi/10.1103/PhysRevA.45.8185.

[15] L. Allen, S.M. Barnett, M.J. Padgett (Eds.), Optical Angular Momentum, Institute of Physics Publishing, ISBN 9780750309011, 2003, URL http://books.google.be/books?id=Vf32PZXJ2gMC.

[16] D.L. Andrews, M. Babiker (Eds.), The Angular Momentum of Light, Cambridge University Press, ISBN 9781107006348, 2012, URL http://books.google.be/books?id=li2bysEqHf0C.

[17] Nana B. Agyei, Flickr — Nanagyei, 2013. URL http://www.flickr.com/photos/nanagyei/6655488913/ [online; accessed 28-June-2013].

[18] M.V. Berry, M.R. Dennis, Knotted and linked phase singularities in monochromatic waves, Proc. R. Soc., Math. Phys. Eng. Sci. 457 (2013) 2251–2263, http://dx.doi.org/10.1098/rspa.2001.0826, URL http://rspa.royalsocietypublishing.org/content/457/2013/2251.abstract, 2001.

[19] M.R. Dennis, Topological singularities in wave fields, PhD thesis, University of Bristol, 2001, URL http://www.bris.ac.uk/physics/media/theory-theses/dennis-mr-thesis.pdf.

[20] D.L. Andrews (Ed.) Structured Light and Its Applications: An Introduction to Phase-Structured Beams and Nanoscale Optical Forces, Elsevier Science, ISBN 9780080559667, 2011, URL http://books.google.be/books?id=BNdCkCXOXX4C.

[21] Jo Verbeeck, He Tian, Gustaaf Van Tendeloo, How to manipulate nanoparticles with an electron beam?, Adv. Mater. (ISSN 1521-4095) 25 (8) (February 2013) 1114–1117, http://dx.doi.org/10.1002/adma.201204206, URL http://www.ncbi.nlm.nih.gov/pubmed/23184603.

[22] Andrew G. Peele, Philip J. McMahon, David Paterson, Chanh Q. Tran, Adrian P. Mancuso, Keith A. Nugent, Jason P. Hayes, Erol Harvey, Barry Lai, Ian McNulty, Observation of an x-ray vortex, Opt. Lett. 27 (20) (Oct 2002) 1752–1754, http://dx.doi.org/10.1364/OL.27.001752, URL http://www.opticsinfobase.org/ol/abstract.cfm?id=70214.

[23] B. Thidé, H. Then, J. Sjöholm, K. Palmer, J. Bergman, T.D. Carozzi, Ya.N. Istomin, N.H. Ibragimov, R. Khamitova, Utilization of photon orbital angular momentum in the low-frequency radio domain, Phys. Rev. Lett. 99 (Aug 2007) 087701, http://dx.doi.org/10.1103/PhysRevLett.99.087701, URL http://prl.aps.org/abstract/PRL/v99/i8/e087701.

[24] Katsuhiko Miyamoto, Sachio Miyagi, Masaki Yamada, Kenji Furuki, Nobuyuki Aoki, Masahito Okida, Takashige Omatsu, Optical vortex pumped mid-infrared optical parametric oscillator, Opt. Express 19 (13) (Jun 2011) 12220–12226, http://dx.doi.org/10.1364/OE.19.012220, URL http://www.opticsinfobase.org/oe/abstract.cfm?uri=oe-19-13-12220.

[25] Bernd Terhalle, Andreas Langner, Birgit Päivänranta, Vitaliy A. Guzenko, Christian David, Yasin Ekinci, Generation of extreme ultraviolet vortex beams using computer generated holograms, Opt. Lett. 36 (21) (Nov 2011) 4143–4145, http://dx.doi.org/10.1364/OL.36.004143, URL http://www.opticsinfobase.org/ol/abstract.cfm?uri=ol-36-21-4143.

[26] K.D. Skeldon, C. Wilson, M. Edgar, M.J. Padgett, An acoustic spanner and its associated rotational Doppler shift, New J. Phys. 10 (1) (2008) 013018, http://dx.doi.org/10.1088/1367-2630/10/1/013018, URL http://stacks.iop.org/1367-2630/10/i=1/a=013018.

[27] Reza Torabi, Zahra Rezaei, The effect of Dirac phase on acoustic vortex in media with screw dislocation, Phys. Lett. A (ISSN 0375-9601) 377 (28–30) (2013) 1668–1671, http://dx.doi.org/10.1016/j.physleta.2013.05.014, URL http://www.sciencedirect.com/science/article/pii/S0375960113004842.

[28] Gregorius C.G. Berkhout, Marco W. Beijersbergen, Method for probing the orbital angular momentum of optical vortices in electromagnetic waves from astronomical objects, Phys. Rev. Lett. 101 (Sep 2008) 100801, http://dx.doi.org/10.1103/PhysRevLett.101.100801, URL http://link.aps.org/doi/10.1103/PhysRevLett.101.100801.

[29] Jian Wang, Jeng-Yuan Yang, Irfan M. Fazal, Nisar Ahmed, Yan Yan, Hao Huang, Yongxiong Ren, Yang Yue, Samuel Dolinar, Moshe Tur, Alan E. Willner, Terabit free-space data transmission employing orbital angular momentum multiplexing, Nat. Photonics (2012), http://dx.doi.org/10.1038/nphoton.2012.138, URL http://www.nature.com/nphoton/journal/v6/n7/full/nphoton.2012.138.html.

[30] Sanjoy Roychowdhury, Virendra K. Jaiswal, R.P. Singh, Implementing controlled NOT gate with optical vortex, Opt. Commun. (ISSN 0030-4018) 236 (4–6) (2004) 419–424, http://dx.doi.org/10.1016/j.optcom.2004.03.036, URL http://www.sciencedirect.com/science/article/pii/S0030401804003013.

[31] J. Durnin, J.J. Miceli, J.H. Eberly, Diffraction-free beams, Phys. Rev. Lett. 58 (Apr 1987) 1499–1501, http://dx.doi.org/10.1103/PhysRevLett.58.1499, URL http://prl.aps.org/abstract/PRL/v58/i15/p1499_1.

[32] J. Verbeeck, P. Schattschneider, S. Lazar, M. Stoger-Pollach, S. Löffler, A. Steiger-Thirsfeld, G. Van Tendeloo, Atomic scale electron vortices for nanoresearch, Appl. Phys. Lett. 99 (20) (2011) 203109, http://dx.doi.org/10.1063/1.3662012.

[33] Konstantin Y. Bliokh, Peter Schattschneider, Jo Verbeeck, Franco Nori, Electron vortex beams in a magnetic field: a new twist on Landau levels and Aharonov–Bohm states, Phys. Rev. X (ISSN 2160-3308) 2 (4) (2012) 041011, http://dx.doi.org/10.1103/PhysRevX.2.041011, URL http://link.aps.org/doi/10.1103/PhysRevX.2.041011.

[34] Konstantin Y. Bliokh, Mark R. Dennis, Franco Nori, Relativistic electron vortex beams: Angular momentum and spin–orbit interaction, Phys. Rev. Lett. 107 (Oct 2011) 174802, http://dx.doi.org/10.1103/PhysRevLett.107.174802, URL http://link.aps.org/doi/10.1103/PhysRevLett.107.174802.

[35] Ruben Van Boxem, Jo Verbeeck, Bart Partoens, Spin effects in electron vortex states, Europhys. Lett. 102 (4) (2013) 40010, http://dx.doi.org/10.1209/0295-5075/102/40010, URL http://stacks.iop.org/0295-5075/102/i=4/a=40010.

[36] Huolin L. Xin, Haimei Zheng, On-column 2p bound state with topological charge $\pm 1$ excited by an atomic-size vortex beam in an aberration-corrected scanning transmission electron microscope, Microsc. Microanal. (ISSN 1435-8115) 18 (7) (2012) 711–719, http://dx.doi.org/10.1017/S1431927612000499.

[37] Benjamin J. McMorran, Amit Agrawal, Ian M. Anderson, Andrew A. Herzing, Henri J. Lezec, Jabez J. McClelland, John Unguris, Electron vortex beams with high quanta of orbital angular momentum, Science (New York, N.Y.) (ISSN 1095-9203) 331 (6014) (January 2011) 192–195, http://dx.doi.org/10.1126/science.1198804, URL http://www.sciencemag.org/content/331/6014/192.abstract.
[38] M.V. Berry, Optical currents, J. Opt. A, Pure Appl. Opt. 11 (9) (2009) 094001, http://dx.doi.org/10.1088/1464-4258/11/9/094001, URL http://stacks.iop.org/1464-4258/11/i=9/a=094001.
[39] G.C.G. Berkhout, Fundamental methods to measure the orbital angular momentum of light, PhD thesis, Leiden University, 2011, URL https://openaccess.leidenuniv.nl/handle/1887/17842.
[40] M.V. Vasnetsov, V.A. Pas'ko, M.S. Soskin, Analysis of orbital angular momentum of a misaligned optical beam, New J. Phys. 7 (1) (2005) 46, http://dx.doi.org/10.1088/1367-2630/7/1/046, URL http://iopscience.iop.org/1367-2630/7/1/046.
[41] Stefan Löffler, Peter Schattschneider, Elastic propagation of fast electron vortices through crystals, Acta Crystallogr. Sect. A 68 (4) (Jul 2012) 443–447, http://dx.doi.org/10.1107/S0108767312013189, URL http://scripts.iucr.org/cgi-bin/paper?S0108767312013189.
[42] I.P. Ivanov, V.G. Serbo, Scattering of twisted particles: Extension to wave packets and orbital helicity, Phys. Rev. A 84 (Sep 2011) 033804, http://dx.doi.org/10.1103/PhysRevA.84.033804, URL http://pra.aps.org/abstract/PRA/v84/i3/e033804.
[43] S.M. Lloyd, M. Babiker, J. Yuan, C. Kerr-Edwards, Electromagnetic vortex fields, spin, and spin–orbit interactions in electron vortices, Phys. Rev. Lett. 109 (Dec 2012) 254801, http://dx.doi.org/10.1103/PhysRevLett.109.254801, URL http://prl.aps.org/abstract/PRL/v109/i25/e254801.
[44] Noa Voloch-Bloch, Yossi Lereah, Yigal Lilach, Avraham Gover, Ady Arie, Generation of electron Airy beams, Nature (ISSN 1476-4687) 494 (7437) (February 2013) 331–335, http://dx.doi.org/10.1038/nature11840, URL http://www.ncbi.nlm.nih.gov/pubmed/23426323.
[45] Peter Schattschneider, M. Stöger-Pollach, J. Verbeeck, Novel vortex generator and mode converter for electron beams, Phys. Rev. Lett. (ISSN 0031-9007) 109 (8) (August 2012) 1–5, http://dx.doi.org/10.1103/PhysRevLett.109.084801, URL http://link.aps.org/doi/10.1103/PhysRevLett.109.084801.
[46] Jo Verbeeck, He Tian, Armand Béché, A new way of producing electron vortex probes for STEM, Ultramicroscopy (ISSN 0304-3991) 113 (October 2011) 83–87, http://dx.doi.org/10.1016/j.ultramic.2011.10.008, URL http://linkinghub.elsevier.com/retrieve/pii/S0304399111002531.
[47] Colin Greenshields, Robert L. Stamps, Sonja Franke-Arnold, Vacuum Faraday effect for electrons, New J. Phys. (ISSN 1367-2630) 14 (10) (October 2012) 103040, http://dx.doi.org/10.1088/1367-2630/14/10/103040, URL http://stacks.iop.org/1367-2630/14/i=10/a=103040.
[48] Giulio Guzzinati, Peter Schattschneider, Konstantin Y. Bliokh, Franco Nori, Jo Verbeeck, Observation of the Larmor and Gouy rotations with electron vortex beams, Phys. Rev. Lett. (ISSN 0031-9007) 110 (9) (February 2013) 093601, http://dx.doi.org/10.1103/PhysRevLett.110.093601, URL http://link.aps.org/doi/10.1103/PhysRevLett.110.093601.
[49] Koh Saitoh, Yuya Hasegawa, Nobuo Tanaka, Masaya Uchida, Production of electron vortex beams carrying large orbital angular momentum using spiral zone plates, J. Electron Microsc. (ISSN 1477-9986) 61 (3) (June 2012) 171–177, http://dx.doi.org/10.1093/jmicro/dfs036, URL http://www.ncbi.nlm.nih.gov/pubmed/22394576.
[50] R. Danev, K. Nagayama, Transmission electron microscopy with Zernike phase plate, Ultramicroscopy (ISSN 0304-3991) 88 (4) (September 2001) 243–252, URL http://linkinghub.elsevier.com/retrieve/pii/S0304399101000882.
[51] R. Danev, H. Okawara, N. Usuda, K. Kametani, K. Nagayama, A novel phase-contrast transmission electron microscopy producing high-contrast topographic images of weak objects, J. Biol. Phys. 28 (4) (2002) 627–635, URL http://www.springerlink.com/index/N5118841393L26XP.pdf.
[52] F. Zernike, Phase contrast, a new method for the microscopic observation of transparent objects, Physica (ISSN 0031-8914) 9 (7) (July 1942) 686–698, http://dx.doi.org/10.1016/S0031-8914(42)80035-X, URL http://linkinghub.elsevier.com/retrieve/pii/S003189144280035X.
[53] F. Zernike, Phase contrast, a new method for the microscopic observation of transparent objects part II, Physica (ISSN 0031-8914) 9 (10) (December 1942) 974–986, http://dx.doi.org/10.1016/S0031-8914(42)80079-8, URL http://linkinghub.elsevier.com/retrieve/pii/S0031891442800798.
[54] K. Schultheiß, F. Perez-Willard, B. Barton, D. Gerthsen, R.R. Schroder, Fabrication of a Boersch phase plate for phase contrast imaging in a transmission electron microscope, Rev. Sci. (ISSN 0034-6748) 77 (3) (2006) 90, http://dx.doi.org/10.1063/1.2179411, URL http://link.aip.org/link/?RSINAK/77/033701/1, http://link.aip.org/link/RSINAK/v77/i3/p033701/s1&Agg=doi.
[55] M.W. Beijersbergen, L. Allen, H. Van der Veen, J.P. Woerdman, Astigmatic laser mode converters and transfer of orbital angular momentum, Opt. Commun. 96 (1–3) (1993) 123–132, URL http://www.sciencedirect.com/science/article/pii/003040189390535D.
[56] T.C. Petersen, M. Weyland, D.M. Paganin, T.P. Simula, S.A. Eastwood, M.J. Morgan, Electron vortex production and control using aberration induced diffraction catastrophes, Phys. Rev. Lett. (ISSN 0031-9007) 110 (3) (January 2013) 033901, http://dx.doi.org/10.1103/PhysRevLett.110.033901, URL http://link.aps.org/doi/10.1103/PhysRevLett.110.033901.
[57] L. Clark, A. Béché, G. Guzzinati, A. Lubk, M. Mazilu, R. Van Boxem, J. Verbeeck, Exploiting lens aberrations to create electron-vortex beams, Phys. Rev. Lett. 111 (Aug 2013) 064801, http://dx.doi.org/10.1103/PhysRevLett.111.064801, URL http://link.aps.org/doi/10.1103/PhysRevLett.111.064801.
[58] Akira Tonomura, Tsuyoshi Matsuda, Ryo Suzuki, Akira Fukuhara, Nobuyuki Osakabe, Hiroshi Umezaki, Junji Endo, Kohsei Shinagawa, Yutaka Sugita, Hideo Fujiwara, Observation of Aharonov–Bohm effect by electron holography, Phys. Rev. Lett. (ISSN 0031-9007) 48 (21) (May 1982) 1443–1446, http://dx.doi.org/10.1103/PhysRevLett.48.1443, URL http://link.aps.org/doi/10.1103/PhysRevLett.48.1443.
[59] C.J. Edgcombe, J.C. Loudon, Use of Aharonov–Bohm effect and chirality control in magnetic phase plates for transmission microscopy, J. Phys. Conf. Ser. (ISSN 1742-6596) 371 (July 2012) 012006, http://dx.doi.org/10.1088/1742-6596/371/1/012006, URL http://stacks.iop.org/1742-6596/371/i=1/a=012006?key=crossRef.7ac987ff9728f0920601ae16f557a3ae.
[60] Akira Tonomura, Applications of electron holography, Rev. Mod. Phys. (ISSN 0034-6861) 59 (3) (July 1987) 639–669, http://dx.doi.org/10.1103/RevModPhys.59.639, URL http://link.aps.org/doi/10.1103/RevModPhys.59.639.
[61] A. Beche, R. Van Boxem, G. Van Tendeloo, J. Verbeeck, Magnetic monopole field exposed by electrons, Nat. Phys. (ISSN 1745-2473) 10 (1) (2014) 26–29, http://dx.doi.org/10.1038/nphys2816.
[62] A.M. Blackburn, J.C. Loudon, Vortex beam production and contrast enhancement from a magnetic spiral phase plate, Ultramicroscopy 136 (2014) 127–143.
[63] Peter Schattschneider, Bernhard Schaffer, I. Ennen, J. Verbeeck, Mapping spin-polarized transitions with atomic resolution, Phys. Rev. B (ISSN 1098-0121) 85 (13) (April 2012) 134422, http://dx.doi.org/10.1103/PhysRevB.85.134422, URL http://link.aps.org/doi/10.1103/PhysRevB.85.134422.
[64] G. Schütz, W. Wagner, W. Wilhelm, P. Kienle, R. Zeller, R. Frahm, G. Materlik, Absorption of circularly polarized X-rays in iron, Phys. Rev. Lett. 58 (Feb 1987) 737–740, http://dx.doi.org/10.1103/PhysRevLett.58.737, URL http://link.aps.org/doi/10.1103/PhysRevLett.58.737.
[65] P. Schattschneider, S. Rubino, C. Hébert, J. Rusz, J. Kunes, P. Novák, E. Carlino, M. Fabrizioli, G. Panaccione, G. Rossi, Detection of magnetic circular dichroism using a transmission electron microscope, Nature (ISSN 1476-4687) 441 (7092) (May 2006) 486–488, http://dx.doi.org/10.1038/nature04778, URL http://www.ncbi.nlm.nih.gov/pubmed/16724061.
[66] P. Schattschneider, I. Ennen, S. Loffler, M. Stoger-Pollach, J. Verbeeck, Circular dichroism in the electron microscope: Progress and applications (invited), J. Appl. Phys. (ISSN 0021-8979) 107 (9) (2010) 09D311, http://dx.doi.org/10.1063/1.3365517, URL http://link.aip.org/link/JAPIAU/v107/i9/p09D311/s1&Agg=doi.
[67] P. Schattschneider, B. Schaffer, I. Ennen, J. Verbeeck, Mapping spin-polarized transitions with atomic resolution, Phys. Rev. B 85 (Apr 2012) 134422, http://dx.doi.org/10.1103/PhysRevB.85.134422.
[68] R.B. Pettit, J. Silcox, R. Vincent, Measurement of surface-plasmon dispersion in oxidized aluminum films, Phys. Rev. B 11 (Apr 1975) 3116–3123, http://dx.doi.org/10.1103/PhysRevB.11.3116, URL http://link.aps.org/doi/10.1103/PhysRevB.11.3116.

[69] Jaysen Nelayah, Mathieu Kociak, Odile Stéphan, F. Javier Garcia de Abajo, Marcel Tencé, Luc Henrard, Dario Taverna, Isabel Pastoriza-Santos, Luis M. Liz-Marzán, Christian Colliex, Mapping surface plasmons on a single metallic nanoparticle, Nat. Phys. (ISSN 1745-2473) 3 (5) (April 2007) 348–353, http://dx.doi.org/10.1038/nphys575, URL http://www.nature.com/nphys/journal/v3/n5/pdf/nphys575.pdf.
[70] Zeinab Mohammadi, Cole P. Van Vlack, Stephen Hughes, Jens Bornemann, Reuven Gordon, Vortex electron energy loss spectroscopy for near-field mapping of magnetic plasmons, Opt. Express (ISSN 1094-4087) 20 (14) (July 2012) 15024–15034, URL http://www.ncbi.nlm.nih.gov/pubmed/22772198.
[71] D.R. Smith, J.B. Pendry, M.C.K. Wiltshire, Metamaterials and negative refractive index, Science 305 (2004) 788–792, URL http://www.sciencemag.org/content/305/5685/788.short.
[72] A. Alù, N. Engheta, Cloaking and transparency for collections of particles with metamaterial and plasmonic covers, Opt. Express 15 (2007) 7578–7590, http://dx.doi.org/10.1088/1464-4258/10/9/093002, URL http://stacks.iop.org/1464-4258/10/i=9/a=093002.
[73] Ebrahim Karimi, Lorenzo Marrucci, Vincenzo Grillo, Enrico Santamato, Spin-to-orbital angular momentum conversion and spin-polarization filtering in electron beams, Phys. Rev. Lett. (ISSN 0031-9007) 108 (4) (January 2012) 044801, http://dx.doi.org/10.1103/PhysRevLett.108.044801, URL http://link.aps.org/doi/10.1103/PhysRevLett.108.044801.